

Lecture Notes in Mechanical Engineering

Eugeniusz Rusiński
Damian Pietrusiak *Editors*

Proceedings of the 14th International Scientific Conference: Computer Aided Engineering

 Springer

Lecture Notes in Mechanical Engineering

Lecture Notes in Mechanical Engineering (LNME) publishes the latest developments in Mechanical Engineering—quickly, informally and with high quality. Original research reported in proceedings and post-proceedings represents the core of LNME. Volumes published in LNME embrace all aspects, subfields and new challenges of mechanical engineering. Topics in the series include:

- Engineering Design
- Machinery and Machine Elements
- Mechanical Structures and Stress Analysis
- Engine Technology
- Aerospace Technology and Astronautics
- Nanotechnology and Microengineering
- Control, Robotics, Mechatronics
- Theoretical and Applied Mechanics
- Dynamical Systems, Control
- Fluid Mechanics
- Engineering Thermodynamics, Heat and Mass Transfer
- Precision Engineering, Instrumentation, Measurement
- Materials Engineering
- Tribology and Surface Technology

To submit a proposal or request further information, please contact the appropriate Springer Editor:

Li Shen at li.shen@springer.com (China)

Dr. Akash Chakraborty at akash.chakraborty@springernature.com (India)

Dr. Leontina Di Cecco at Leontina.dicecco@springer.com (all other Countries)

Please check the Springer Tracts in Mechanical Engineering at <http://www.springer.com/series/11693> if you are interested in monographs, textbooks or edited books.

To submit a proposal, please contact Leontina.dicecco@springer.com and Li.shen@springer.com.

Indexed by SCOPUS. The books of the series are submitted for indexing to Web of Science.

More information about this series at <http://www.springer.com/series/11236>

Eugeniusz Rusiński · Damian Pietrusiak
Editors

Proceedings of the 14th
International Scientific
Conference: Computer Aided
Engineering

 Springer

Editors

Eugeniusz Rusiński
Faculty of Mechanical Engineering
Wrocław University of Science
and Technology
Wrocław, Poland

Damian Pietrusiak
Faculty of Mechanical Engineering
Wrocław University of Science
and Technology
Wrocław, Poland

ISSN 2195-4356 ISSN 2195-4364 (electronic)
Lecture Notes in Mechanical Engineering
ISBN 978-3-030-04974-4 ISBN 978-3-030-04975-1 (eBook)
<https://doi.org/10.1007/978-3-030-04975-1>

Library of Congress Control Number: 2018967408

© Springer Nature Switzerland AG 2019

This work is subject to copyright. All rights are reserved by the Publisher, whether the whole or part of the material is concerned, specifically the rights of translation, reprinting, reuse of illustrations, recitation, broadcasting, reproduction on microfilms or in any other physical way, and transmission or information storage and retrieval, electronic adaptation, computer software, or by similar or dissimilar methodology now known or hereafter developed.

The use of general descriptive names, registered names, trademarks, service marks, etc. in this publication does not imply, even in the absence of a specific statement, that such names are exempt from the relevant protective laws and regulations and therefore free for general use.

The publisher, the authors and the editors are safe to assume that the advice and information in this book are believed to be true and accurate at the date of publication. Neither the publisher nor the authors or the editors give a warranty, express or implied, with respect to the material contained herein or for any errors or omissions that may have been made. The publisher remains neutral with regard to jurisdictional claims in published maps and institutional affiliations.

This Springer imprint is published by the registered company Springer Nature Switzerland AG
The registered company address is: Gewerbestrasse 11, 6330 Cham, Switzerland

Contents

Numerical Analysis and Tests on Selected Dynamic Parameters of Shooting Stand Frame	1
Paweł Abratowski	
The Numerical-Experimental Studies of Stress Distribution in the Three-Arm Boom of the Hybrid Machine for Demolition Works	8
Jakub Andruszko and Damian Derlukiewicz	
Analysis of the Causes of Fatigue Cracks in the Carrying Structure of the Bucket Wheel in the SchRs4600 Excavator Using Experimental-Numerical Techniques	15
Jakub Andruszko, Przemysław Moczko, Damian Pietrusiak, Grzegorz Przybyłek, and Eugeniusz Rusiński	
Numerical-Experimental Approach to the Design of the Mounting System for Fast Clamping of the Equipment of the Electrical Demolition Machine	29
Jakub Andruszko and Eugeniusz Rusiński	
Use of Rapid Manufacturing Methods for Creating Wind Tunnel Test Models	36
Piotr Araszkiwicz	
Statistical Analysis of Loading for the Simulation of Belt Conveyor-Based Transportation System	44
Piotr J. Bardziński, Witold Kawalec, and Robert Król	
Determining Power Losses in the Cycloidal Gear Transmission Featuring Manufacturing Deviations	55
Sławomir Bednarczyk	
Structural Analysis of Historical Masonry Church Construction	64
Łukasz Bednarz, Artur Górski, Jerzy Jasieńko, and Eugeniusz Rusiński	

Use of Artificial Neural Networks for the Estimated Prediction of Haul Trucks Operating States	72
Przemysław Bodziony, Rafał Kudelski, Michał Patyk, and Zbigniew Kasztelewicz	
Fatigue Life Calculation with the Use of the Energy Parameter for the Elastic Material State in the Spectral Method	80
Michał Böhm and Tadeusz Łagoda	
Numerical and Experimental Investigation of Bolted Connections with Blind Rivet Nuts	88
Cezary Borowiecki, Artur Iluk, Paweł Krysiński, Eugeniusz Rusiński, and Marek Sawicki	
Numerical Model of an External Gear Pump and Its Validation	96
Rafał Cieśllicki, Jacek Karliński, and Piotr Osiński	
Modelling of a Vertical Axis Wind Turbine Blade Adjusting Cam Wheel	104
Michał Ćmil	
Vibration Analysis of an Exhaust Fan in the Exhaust Gas Duct of a Power Plant Unit	112
Jerzy Czmochowski, Przemysław Moczko, Maciej Olejnik, and Damian Pietrusiak	
A Sub-modeling Approach for Building Numerically Efficient Discrete Model for Shape Optimization - A Case Study	120
Piotr Danielczyk	
Identification of Influence of Part Tolerances of 2PWR-SE Pump on Its Total Efficiency Taking into Consideration Multi-valued Logic Trees	128
Adam Deptuła, Piotr Osiński, and Marian A. Partyka	
Application of Decision Logical Trees and Predominant Logical Variables in Analysis of Automatic Transmissions Gearboxes	136
Adam Deptuła and Marian A. Partyka	
Structural Analysis of Live Steam Pipelines in the Context of the Replacement System Hanger	144
Tomasz Dobosz, Jakub Dominiak, Michał Paduchowicz, and Artur Górski	
Application of Fem Method for Modeling and Strength Analysis of Feed Elements of Vibroscreen	155
Mikhail Doudkin, Alina Kim, and Vadim Kim	
Numerical Investigations of the Influence of Seismic Vibrations on the Transformer Structure	163
Sławomir Duda, Sławomir Kciuk, Jacek Gniłka, and Tomasz Kaszyca	

Aspects of the Cryogenic Equipment Mechanical Calculations on an Example of the FRESKA2 Cryostat	175
P. Duda, J. Polinski, M. Grabowski, A. V. Craen, V. Parma, and M. Chorowski	
Modelling Machine Tool Rocking Vibrations Using Reduced Order Models	183
Paweł Dunaj, Stefan Berczyński, and Michał Dolata	
Algorithmic Method of Constructional Features Selection of the Module System of Hydraulic Cylinders Utilized in National Mining Industry	191
Piotr Gendarz, Aleksander Gwiazda, and Lothar Kroll	
Animation and Simulation as the Base of Technical Means Systems Verification	199
Piotr Gendarz, Aleksander Gwiazda, and Lothar Kroll	
Integration of Constructional Features Selection and Construction Description	207
Piotr Gendarz, Aleksander Gwiazda, and Lothar Kroll	
Spatial Reduced Dynamic Model of a Bucket Wheel Excavator with Two Masts	215
Nebojša Gnjatović, Srđan Bošnjak, and Nenad Zrnić	
Innovative Rotor of Water Turbine Save for River Ecosystem	236
Aleksander Górnjak, Anna Janicka, Joanna Mikołajczak, Maria Skrętowicz, Dariusz Piętas, Radosław Włostowski, and Maciej Zawiślak	
Analysis of Composite Structure Effect on Radio-Frequency Characteristics of the RFID Tag	242
Piotr Górski, Jacek Lewandowski, Paweł Krowicki, and Tadeusz Lewandowski	
Design of the Vehicle Frontal Protection System for Emergency Services	252
Artur Górski, Tadeusz Lewandowski, Wiktor Słomski, and Mariusz Ptak	
Application of CFD Methods in Determining the Implementation Areas of Protective Coatings Used to Improve a Water Turbine Lifetime	259
Dominika Grygier, Anna Janicka, Agnieszka Kocikowska, Alina Rudiak, Małgorzata Rutkowska-Gorczyca, Krzysztof Sobczak, and Maciej Zawiślak	

Comparison of Stress Distribution Between Geometrically Corrected Wire-Raceway Bearings and Non-corrected Wire-Raceway Bearings	266
Dominik Gunia and Tadeusz Smolnicki	
Modeling of the Constrain of the Foot with the Bicycle Pedal While Driving with a Constant Cadence	276
A. Handke and J. Bałchanowski	
Computer Aided Diagnosis and Prediction of Mechatronic Drive Systems	284
Mariusz Piotr Hetmańczyk and Jerzy Świder	
Experimental Investigation of Load Carrying Structure of 155 mm Self-propelled Howitzer During Test Fire	293
Artur Iluk and Mariusz Stańco	
Statistical Evaluation of an Exhaust Gas Mixture for Photocatalytic Reactor Test-Station Improvement	301
Anna Janicka, Maciej Zawisłak, Aleksander Górniak, and Daniel Michniewicz	
Diagnostic Procedure of Bucket Wheel and Boom Computer Modeling – A Case Study Revitalization Bucket Wheel and Drive of BWE SRs2000	310
Predrag Jovančić, Dragan Ignjatović, Taško Maneski, Dragan Novaković, and Časlav Slavković	
Comparative Analysis of Experimental and Numerical Evaluation of Strength of a Boom of the Underground Loader	319
Jacek Karliński and Paulina Działak	
Sustainable Development Oriented Belt Conveyors Quality Standards	327
Witold Kawalec and Robert Król	
The Numerical Calculation Module for Piston Rings & Cylinder of Combustion Engine	337
Andrzej Kaźmierczak and Marcin Tkaczyk	
Numerical Simulation of Residual Stress Induced by Welding of Steel-Aluminum Transition Joint	346
M. Kowalski and M. Bohm	
Designing of the Structure Elements Being Bent from the Fatigue Life Point of View	353
Justyna Koziarska, Andrzej Kurek, and Tadeusz Łagoda	

Selection of Geometric Features of V-Belt Transmission Through Multi-criteria Analysis	361
Michał Krawiec	
Design, Strength Analysis and Destructive Testing Rotating Discs	370
Kamil Krot and Piotr Górski	
Methodology for Assessing Blast Threat of EOD Personnel	379
Edyta Krzystała, Krzysztof Kawlewski, Sławomir Kciuk, Grzegorz Bienioszek, and Tomasz Machoczek	
Numerical Modelling of Cylindrical Test for Determining Jones – Wilkins - Lee Equation Parameters	388
Michał Kucewicz, Paweł Baranowski, Jerzy Małachowski, Waldemar Trzcziński, and Leszek Szymańczyk	
Strain-Life Fatigue Curves on the Basis of Shear Strains from Torsion	395
Andrzej Kurek, Marta Kurek, and Tadeusz Łagoda	
The Use of Selective Laser Melting as a Method of New Materials Development	403
Tomasz Kurzynowski, Konrad Gruber, and Edward Chlebus	
Processing of Magnesium Alloy by Selective Laser Melting	411
Tomasz Kurzynowski, Andrzej Pawlak, and Edward Chlebus	
Strength Analysis of the Multi-tasking Car Trailer	419
Piotr Ladra and Bogdan Posiadała	
Correlation of Wear and Time in Research Conducted at Concentrated Point Contact	427
Tadeusz Leśniewski	
Feasibility Study on Location Monitoring of Technical Objects During Operational Phase	433
Jacek Lewandowski, Piotr Górski, Tadeusz Lewandowski, Paweł Krowicki, and Maciej Merek	
Bending Strength of a Thick-Walled Composite in a Thermoplastic Matrix	446
Karolina Łagoda, Andrzej Kurek, Anna Kulesa, Wojciech Błażejewski, and Tadeusz Łagoda	
Computer Aided Design of Wood Pellet Machines	454
Marek Macko and Adam Mroziński	

CAE/FDM Methods for Design and Manufacture Artificial Organs for Exercises Purposes	462
Marek Macko, Zbigniew Szczepański, Dariusz Mikołajewski, Joanna Nowak, Emilia Mikołajewska, and Jacek Furtak	
Parameter Selection Rules for Energy-Absorbing Element of the Spring Type Based on Numerical Analysis	470
Adrian Małczuk	
Strength and Fatigue Analysis of the Welding Connection on the Compressed Air Tank	478
Paweł Maślak and Tadeusz Smolnicki	
Welding Procedure in Designing Carrying Structures of Machines	485
Robert Misiewicz, Grzegorz Przybyłek, and Jędrzej Więckowski	
Numerical and Experimental Testing of the WLS Series Axial Fans Used for Local Ventilation of Underground Excavations	497
Przemysław Moczko, Jędrzej Więckowski, and Piotr Odyjas	
Integration of Motion Capture Data Acquisition with Multibody Dynamic Simulation Software for Nordic Walking Gait Analysys	510
A. Muraszkowski, J. Szrek, S. Wudarczyk, J. Bałchanowski, R. Jasiński, B. Pietraszewski, and M. Woźniewski	
Conceptual Design and Concept Development of Compressed Biogas Transport System Using CAD/CAE	518
Marek Mysior, Sebastian Koziółek, and Bartosz Pryda	
Determination of the Bucket Wheel Suspension Stiffness	527
Marek Onichimiuk, Marian Wygoda, Adam Bajcar, Damian Pietrusiak, and Przemysław Moczko	
Numerical Analysis of the Crash-Test Platform	537
Krzysztof Podkowski, Zbigniew Barszcz, and Patryk Melańczuk	
Head-to-Bonnet Impact Using Finite Element Head Model	545
Mariusz Ptak, Dorota Czerwińska, Johannes Wilhelm, Fábio A. O. Fernandes, and Ricardo J. Alves de Sousa	
Numerical and Experimental Analysis of Polyethylene Material Compositions for Use in Joint Endoprosthesis	556
Anita Ptak, Piotr Kowalewski, and Żaneta Michalska	
Numerical Simulation of a Motorcycle to Road Barrier Impact	565
Mariusz Ptak, Johannes Wilhelm, Olga Klimas, Grzegorz Reclik, and Leszek Garbaciak	

Use of Radiography to Identify the Gangue 574
 Agnieszka Pustułka and Tadeusz Leśniewski

**Qualitative Evaluation of Modeling the Aramid Fabric
 Elementary Cell in the Piercing Process with a 9 mm Full Metal
 Jacket Projectile** 581
 Dariusz Pyka, Joanna Pach, Mirosław Bocian, and Krzysztof Jamroziak

**Development of Auxiliary Gas Protection During Laser Cladding
 on the Axisymmetric Ti6Al4V Component** 591
 Przemysław Radkiewicz, Piotr Koruba, and Jacek Reiner

Structural Analysis of Composite Scooter Monocoque 599
 Igor Rogacki, Eugeniusz Rusiński, and Marek Sawicki

**Analysis of Material Properties Base on Fluid Structure
 Interaction Simulation** 611
 Robert Roszak, Daniela Schob, Holger Sparr, and Matthias Ziegenhorn

Structural Analysis of PVC-CF Composite Materials 619
 Przemysław Rumianek, Piotr Żach, Radosław Nowak, and Piotr Kosiński

**Selected Problems of Fatigue Testing of Automotive
 Drive Shafts** 627
 Eugeniusz Rusiński, Tomasz Dobosz, Fabian Grendysz,
 and Przemysław Moczko

**Selected Problems of Strength Calculation of Power Boiler
 Steam Superheater** 636
 Eugeniusz Rusiński, Artur Górski, Michał Attinger, Jerzy Czmochowski,
 and Michał Paduchowicz

Simulation of Cavitation Participation in the Water Treatment 645
 Lech J. Sitnik

**Modeling of Liquid Exchange Process in a Hydraulic Cylinder
 Chamber in the Aspect of Power System Design** 653
 Tomasz Siwulski, Urszula Warzyńska, Łukasz Moraś, Piotr Rosikowski,
 and Paweł Pac

**Assessment of Atmospheric Air Quality in the Area
 of the Legionow Square in Wrocław** 661
 Maria Skretowicz and Anna Galas-Szpak

**Application of Multi-vector Iteration to Identification
 of Load Distribution in Slewing Bearing of Excavator** 669
 Michał Smolnicki and Tadeusz Smolnicki

Numerical Modelling of Thermal and Mechanical Properties of Construction Elements in a Heat Storage Unit with Phase Change	678
Daniel Smykowski, Tomasz Tietze, Piotr Szulc, and Kazimierz Wójs	
Thermal Evaluation of Operation of Disc Brakes Made of Selected Materials	688
Justyna Sokolska and Piotr Sokolski	
Problems of Strength Estimation of the Vulnerable Zones in the Tools of Hydraulic Hammers for Mining	696
Marek Sokolski and Piotr Sokolski	
Thermo-Mechanical Material Modelling for Cyclic Loading a Generalized Modelling Approach to Different Material Classes	705
Holger Sparr, Daniela Schob, and Matthias Ziegenhorn	
Kinematic Analysis of a Mobile Robot While Overcoming Curb	712
Przemysław Sperzyński and Bogusz Lewandowski	
The Impact of Piston Design on Thermal Load of Internal Combustion Engine	720
Zbigniew J. Sroka and Kacper M. Kot	
Analysis of the Influence of Leaf Geometry on Stiffness and Effort of the Heavy-Duty Spring	728
Mariusz Stańco	
Failure Analysis of a Damaged U-Bolt Top Plate in a Leaf Spring	736
Mariusz Staco, Paulina Działak, and Maciej Hejduk	
Development of Measuring Points for Experimental Tests of Loads on the Driving Axle of a City Bus	744
M. Stańco, A. Górski, and D. Derlukiewicz	
Static and Dynamic Tests of Suspension System Heavy Off-road Vehicle	752
M. Stańco, A. Iluk, and M. Sawicki	
Studies of Resistances of Natural Liquid Flow in Helical and Curved Pipes	759
Michał Stosiak, Maciej Zawiślak, and Bohdan Nishta	
Designing Gear Pump Bodies Using FEM	767
J. Stryczek, K. Biernacki, and J. Krawczyk	
Modal Analyses of Small Wind Turbine	784
Tomasz Szafrański, Jerzy Malachowski, and Krzysztof Damaziak	

Force Measurement Module for Mechatronic Nordic Walking Poles	790
Jarosław Szrek, Artur Muraszkowski, Jacek Bałchanowski, Sławomir Wudarczyk, Ryszard Jasiński, Tadeusz Niebudek, and Marek Woźniewski	
Modelling of Thermal and Flow Processes in a Thermal Energy Storage Unit with a Phase-Change Material	795
Piotr Szulc, Daniel Smykowski, Tomasz Tietze, and Kazimierz Wójs	
FEM Analysis of Mini-Plate for Osteosynthesis of Mandibular Fractures Dedicated for Future Manufacturing with Additive Technologies (AM)	806
Patrycja Szymczyk, Małgorzata Rusińska, Grzegorz Ziółkowski, Beata Łoś, and Edward Chlebus	
Correlation of Hydraulic and Pneumatic Tightness for Brake Fluid Reservoir Non Return Valve	814
Maciej Wnuk and Artur Iluk	
Linked a Priori and a Posteriori Models of Composite Manufacturing Process Chain	823
J. Wollmann, D. R. Haider, M. Krahl, A. Langkamp, and M. Gude	
Simulation of a System for Controlling Atmosphere in Furnace Used to Heating of Blanks	829
Ireneusz Wróbel and Krzysztof Sikora	
Kinematic Design of the Drilling Rig Boom	836
Sławomir Wudarczyk, Jacek Bałchanowski, and Jarosław Szrek	
Modeling of Energy Recovery from Lowering the Fork Carriage Using the Adams System	844
P. Zajac and S. Kwasniowski	
Modeling of the Energy Consumption of a Forklift Truck Using the Matlab Simulink System	851
P. Zajac and P. Skorupski	
Brown Coal – Today and in the Future	858
Sławomir Zawada	
Author Index	871



Numerical Analysis and Tests on Selected Dynamic Parameters of Shooting Stand Frame

Paweł Abratowski^(✉)

Institute of Aviation, Transport Systems Department, Al. Krakowska 110/114,
02-256 Warsaw, Poland
pawel.abratowski@ilot.edu.pl

Abstract. To build a machine gun on a helicopter board sufficiently rigid frame of shooting stand is required. The construction of the frame ensures changing a shoot direction in the vertical and rotation in the horizontal plane. The frame is hinged and can be pivoted to the inside of a helicopter. The frame design requires dynamic analysis and appropriate laboratory tests. The paper presents calculated results of the systems response to the applied dynamic loads in comparison to the laboratory tests results.

Keywords: FEM dynamic analysis · Stand frame tests · Clearance modeling

1 Introduction

One of the topics implemented by Institute of Aviation was laboratory tests and numerical analysis of the frame of a shooting stand designed by customer of the institute. Preliminary analysis of a similar new designed column stand for aircraft multi-barrel machine gun was also carried out and published in [2]. Similar shooting stand frames are described also in [1]. The frame, which is the subject of this article, is mounted in emergency exit of Mi-17 helicopter. The frame consist of welded steel pipes, steel sheets and hinges as one part. The hinges allow the frame to be pivoted to inside of the helicopter. On the other side the special pin (on a spring) makes it possible to lock the frame in working position. A rotary base is attached to the frame on which the machine gun is mounted. 7.62 mm multi-barrel machine gun weights 30 kg. The frequency of shots is 70 Hz. The steel 30HGSA is used as the material of the structure. The frame construction with a machine gun is shown on Fig. 1.

Laboratory frame test included:

- Static test
- Dynamic test – damped free vibrations test. The machine gun replaced by mass substitute
- Dynamic test – load of dynamic force. The loads has been realised in 3-seconds cycles. The assumed firing frequency of the machine gun was 70 Hz but there was

applied 35 Hz due to the limitations of the test stand. The structure was loaded calculated force as if the machine gun was mounted, therefore the tests were performed without mass of the gun.

The purpose of the analysis is to examine the system's response to a static and dynamic load and compare it to the test results. Fatigue tests and calculations are not taken into account in this article.

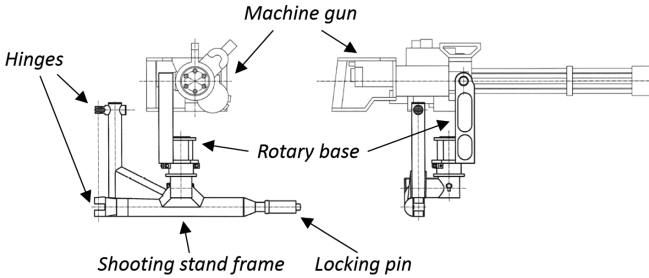


Fig. 1. Shooting stand frame with the machine gun

2 The Loads and Numerical Model

The dynamic force, shown in Fig. 2, is used directly from the laboratory test stand [3]. The duration of the dynamic force is limited to 1.5 s. Two variants model are made: variant 1 – without clearance, variant 2 – modification of variant 1 with clearance simulation. Geometric model with the method of applying support and load is shown in Fig. 3. The loads variants used for analysis are shown in Table 1. The value of U_1 is maximum absolute value obtained in the test. This is initial displacement boundary condition.

Table 1. Loads

Analysis variant	Name	Description	Value
Static analysis, nonlinear	Load 1	Static force	$F1 = -1329 \text{ N}$
	Load 2	Static force	$F2 = 818 \text{ N}$
Dynamic analysis, free vibrations	Load 3	Displacement	$U_1 = -0.253 \text{ mm}$
Dynamic analysis, time dependent force load	Load 4	Course of calculated dynamic force $f(t)$	Fig. 2

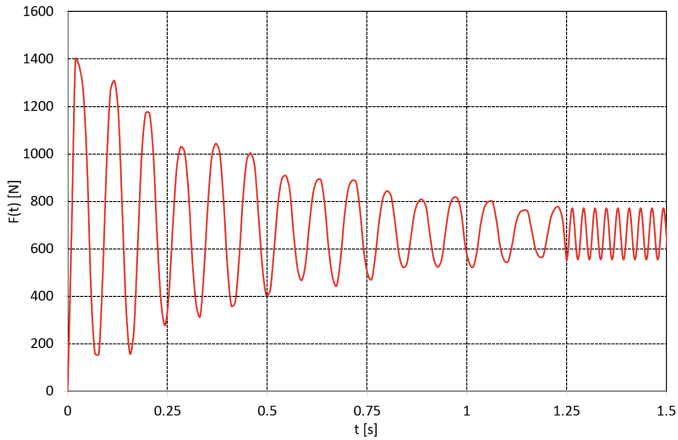


Fig. 2. Dynamic force $F(t)$ [N]

The numerical model including the frame together with rotary base is developed using ANSYS program. The mesh model is shown on Fig. 4. The FE models are developed using 4-nodal shell elements (6 degrees of freedom at each node), 8-nodal solid elements (4 degrees of freedom at each node), beam elements (6 degrees of freedom at each nodes), mass element (the machine gun, forced vibrations) and 2-nodal contact element for clearance modeling. Simplified contact model is shown in Fig. 3.

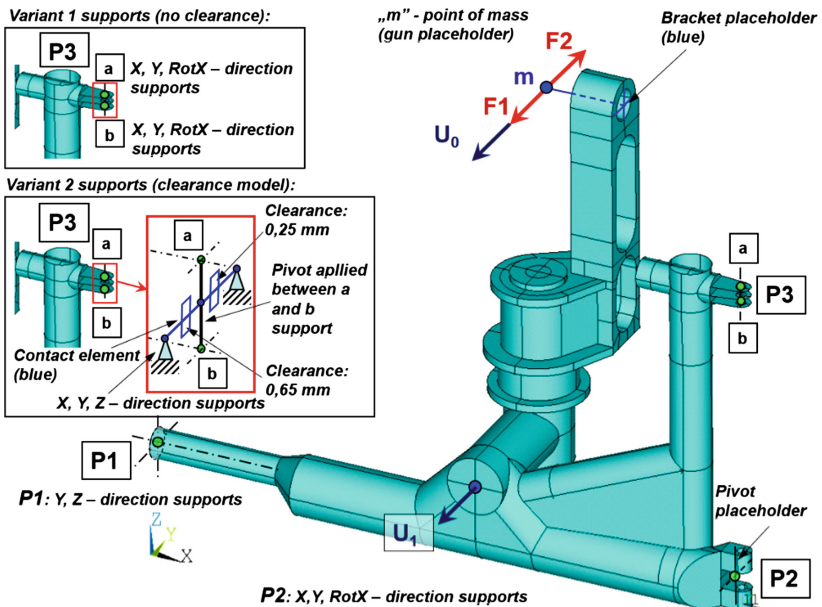


Fig. 3. Loads, supports and clearance model

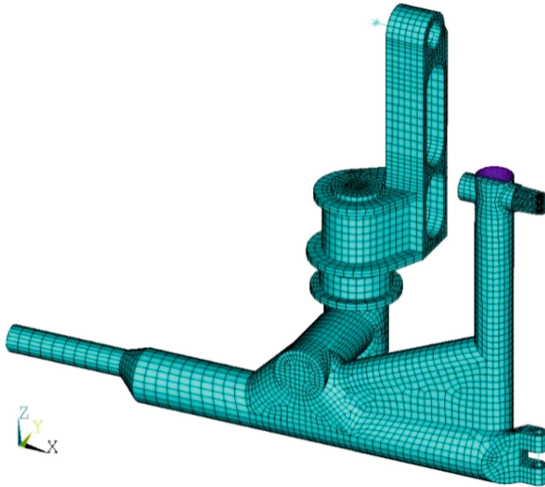


Fig. 4. FE discretization

3 Static Analysis

Static nonlinear analysis is performed using two models (as mentioned in Chap. 2). First – without clearance in supports and second – the clearance is applied in the P3 support (Fig. 3). The clearance values is determined based on the results of the tests and the model without clearance. The clearance is selected so as obtain approximate U_0 displacement to the tested model. The chart shown in Fig. 5 shows displacement U_0 (Fig. 3) for the test results [3], model without clearance results and model with applied clearance.

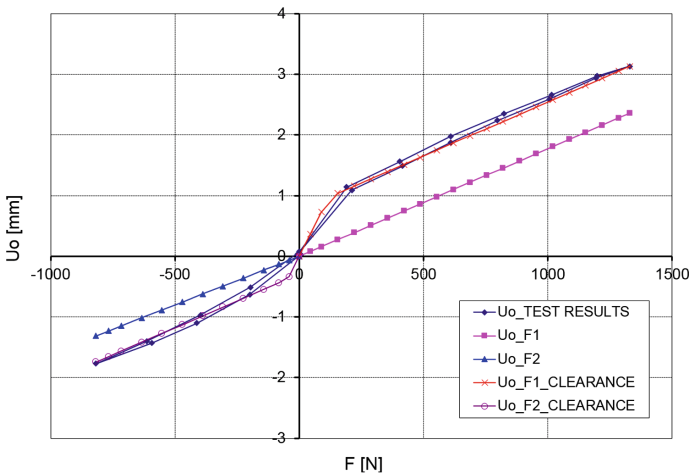


Fig. 5. U_0 [mm] displacement static results

4 Dynamic Analysis

Dynamic transient implicit analysis is performed using Newmark method [4]. Default Newmark parameters in Ansys are applied. In the frame structure the Rayleigh model damping [5] is applied:

$$[C] = \alpha[M] + \beta[K], \quad (1)$$

where, $\alpha = 0$, three coefficients β are applied: 0.0007, 0.001 and 0.0015.

Free vibration analysis is performed using model with mass substitute of the gun $m = 30$ kg (as mentioned in Chap. 1). The initial displacement is applied such that U_1 is equal to the maximum amplitude of the test result. The results (shown in Fig. 6) shows U_1 time dependent displacements for three β damping coefficients in comparison to the test results [3]. The test results are also published in [6].

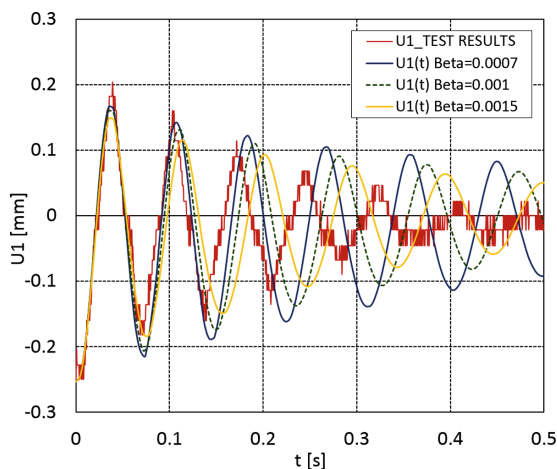


Fig. 6. Free vibrations. U_1 [mm] displacement results

The chart shows the difference in the course of the damping between the test and calculations results. It can be seen that the result for assumed $\beta = 0.0015$ is the nearest to the test result (on the negative side), whereas the vibration period increases at the fastest rate.

The frame analysis with dynamic force load is performed without the mass (as in laboratory tests). During the tests, the load of time dependent force was performed in series. There were performed above 85000 series. Due to the limited volume of this article, there was selected one typical test result for comparison. The test and calculation results for the $\beta = 0.0015$ coefficient are shown in Fig. 7.

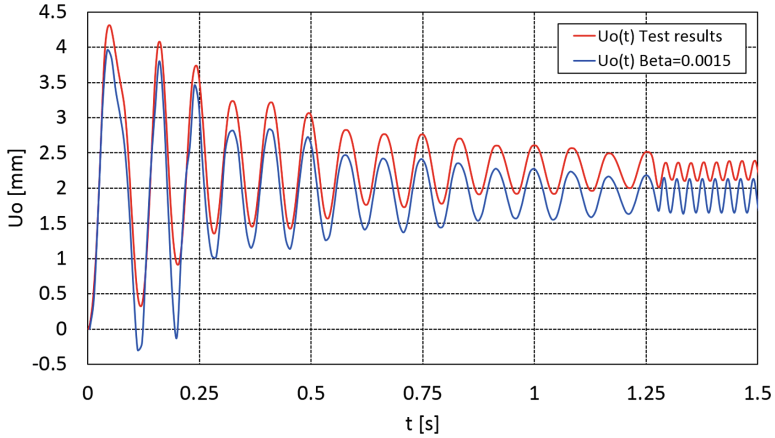


Fig. 7. U_0 displacement results [mm]

The chart shows the difference in the maximum amplitude values between test and calculations results. The minimum difference for the maximum absolute displacements is 0.241 mm at about $t = 0.05$ s. At steady state (from about $t = 1.25$ s) the difference in maximum displacement is 0.227 (4%), whereas the amplitude of the calculated results is approximately twice the tests.

The Fig. 8 shows the frame on the test bench with marked characteristic measuring points.

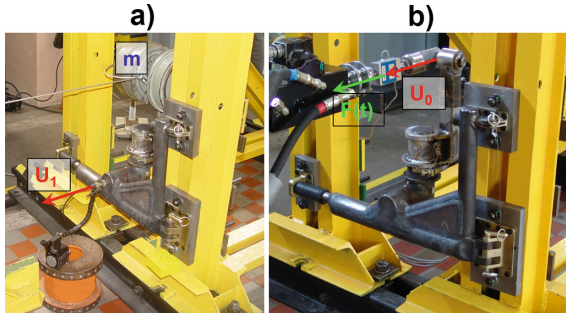


Fig. 8. The frame mounted on the test bench. Configuration of the test stand for: (a) – free vibrations test, (b) – tests with dynamic loads

5 Summary and Conclusions

1. Static analysis shows high accuracy in comparison to test results, especially model stiffness. There is possible to set the clearance value in the frame at a high level of accuracy basing on comparison of the calculations and the test results.

2. Free vibrations analysis shows the differences. It is possible to set the damping coefficient, whereby with a higher damping factor, the vibration period increases faster. In the next step of the research, a non-linear damping coefficient will be applied.
3. Although the value of the clearance may be set with the high accuracy, the calculated results differ from the test results. The differences between maximum and minimum displacements may be caused the different masses between real and numerical model. The mass and stiffness of the dynamometer (shown in Fig. 8b) are not take into account. It can affect the dynamic calculation results. The influence of mass and stiffness of the dynamometer on dynamic results should be checked.

References

1. Сушков С, Струцкий ВГ, Данеко АИ, Полковников ВА, Тимашев ИВ (1998) Авиационные артиллерийские установки, Москва, Издательство МАИ. ISBN 5-7035-1383-9
2. Abratowski P, Krasoń W, Barnat W, Gnarowski W (2017) Dynamic analysis of column stand for aircraft multi-barrel machine gun with consideration of bearing clearance. In: Lecture notes in mechanical engineering. Springer International Publishing AG
3. Gębski M, Raport z badań próby stanowiska strzeleckiego 7.62 mm WPKM (7.62 Wielolufowy Pokładowy Karabin Maszynowy), raport wewnętrzny Instytutu Lotnictwa nr CBMK/LM1/51073.01-04/1/2010
4. Bushby HR, Staab GH (2008) Structural dynamics: concepts and applications. CRC Press
5. ANSYS 14 (2005) Manual
6. Abratowski P, Krasoń W, Barnat W, Gnarowski W (2017) The overview of construction and selected aspects of testing mounting frames of aircraft machine guns. J Sci Gen 49(1): 183. Tadeusz Kosciuszko Military Academy of Land Forces, Wrocław



The Numerical-Experimental Studies of Stress Distribution in the Three-Arm Boom of the Hybrid Machine for Demolition Works

Jakub Andruszko^(✉) and Damian Derlukiewicz

Faculty of Mechanical Engineering,
Department of Machine Design and Research,
Wrocław University of Science and Technology, Łukasiewicza 5, 50-370
Wrocław, Poland
{jakub.andruszko,damian.derlukiewicz}@pwr.edu.pl

Abstract. An electric machine for construction works is a multi-functional, remote-controlled demolition robot which is designed to be operated in hard work condition where the human being is not recommended due to high risks resulting, for example high dust content, high temperature or noise. In such machines, their parts wear out very quickly. The article presents the approach to validate the project assumptions using experimental and numerical studies. The experimental studies provided the information about the adverse efforts and frequency states of the machine. The numerical calculation consigns the information about the stress distribution in the whole arm working system.

Keywords: Demolition machine · Electric machine · Arm working system · Numerical-experimental studies · Construction works · High-speed camera · Testing · Finite element method

1 Introduction

As a result of the growing demand for automating the process of demolishing building structures and for the removal of rocks and spoil in the mid-nineteenth century, the development of specialized demolition machines took place. Over time and the need to automate the process of demolition, the strength of human muscles has been changed to light machines and then to heavy machines such as excavators equipped with specialized equipment for demolition. Over the years, entrepreneurs have at their disposal cranes or excavators with a suspended sphere, excavators with specialized arms and a mounted hydraulic hammer. The most crucial moment was the provision of an electric demolition machine, whose dimensions allowed for demolition of elements inside buildings. The use of electric demolition machines allows to optimize the working environment of the machine in terms of operator safety. The use of electric drive allows the machine to move in closed rooms without causing it to become smoky or producing harmful exhaust gases as in the case of machines with the use of an exhaust system [9] (Fig. 1).



Fig. 1. Visualization of the electric D-REX demolition machine

2 Experimental Studies

Several measurement methods can be used for measurements in the machine's working environment. The most often used is a strain gauges, and to eliminate measurement errors in its application resulting from environmental conditions and for validation of the computational model to determine resonant frequencies a high-speed camera can be used [1, 2]. Comparing the determined resonance frequencies with those calculated in the FEM analysis, we gain assurance of the adopted assumptions and simplifications in the construction of a computational model [7]. Due to the need to eliminate the harmful effects of the environment on the results of measurements, a high-speed camera was used.

The measurements were carried out in the working environment of the machine and the element which has been subjected to the breaking process was a block of reinforced concrete, which was a fragment of the foundation of the building. In the case of such positioning of the machine, the maximum possible extension of the cylinders was chosen so that the position of the arms could generate the greatest possible torque at the rotating element of the working system. This case is the worst possible case of the work system in this environment. Figure 2 shows the machine in the work environment together with the prepared measuring stand and the basic parameters of the measurement.



Speed of the camera: 10 000 frames per second

Density of sampling of displacement signal: 0.001 m

Fig. 2. Work environment of the machine, test stand and parameters of the measurement

The measurement concerned the work of the hammer, which hit the concrete block, destroying the forged material. The obtained graph of displacement in relation to time presents the vertical component of motion, the horizontal one was negligibly small, so it was decided not to plot its dependence and not to apply it in the simulation process (Fig. 3) [3].

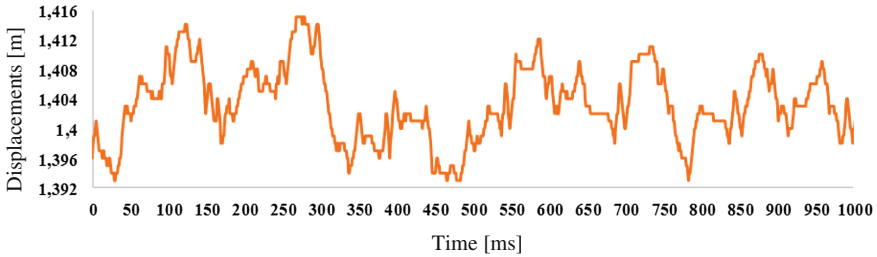


Fig. 3. Displacement of the fastening system point during breaking

To obtain the correct results, image scaling was performed by determining the actual distance between two points in the mounting system (distance between pins). Thanks to the TEMA Motion software and the registered image was analyzed. Having the measured displacement of the system and the time of the measurement, the speed of the desired point was determined and then its acceleration. The minimum size of the pixel can be 20 μm , and a change in its size can affect the measurement error. In the measuring the natural frequency of the system, acceleration diagrams were determined from time, and then the relationship between acceleration and frequency was plotted thanks to FFT analysis [4] (Fig. 4).

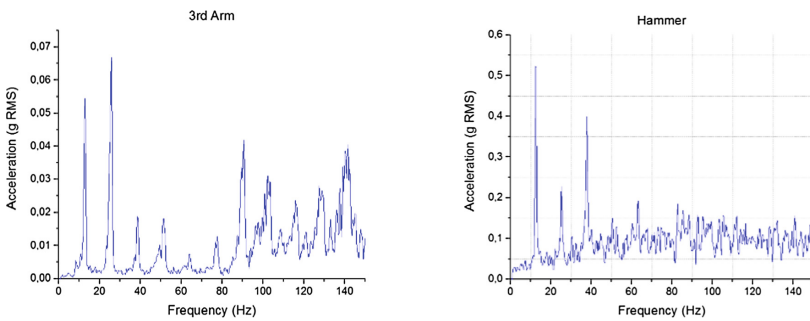


Fig. 4. The spectrum of the signal recorded on the last arm and hammer during operation in the range up to 150 Hz

3 Computational Model

In order to check the strength of the designed working system, a discrete model was built [6, 8]. Discrete model was built on the basis of shell and beam-rod and rigid elements. The geometrical assembly model is built without pins, actuators and additional connecting elements that is modeled as connections in the process of building a computational model [5]. The discrete model with simplifications used in the form of additional elements and named parts is shown in Fig. 5.

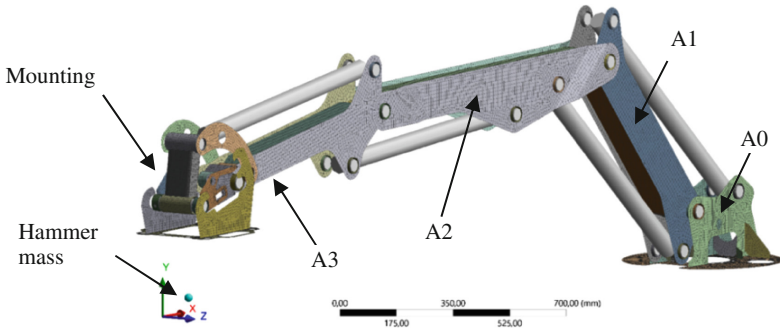


Fig. 5. Discrete model of the working system

Numerical analyzes were carried out in two stages: in the first stage, the resonance frequencies of the working system were determined in order to validate the calculation model with the real model, while in the second stage the effort of the working system, with the given displacement, was analyzed.

4 Results of the Simulation

To assess the correctness of the preparation of the computational model, the results of measurements using a high-speed camera and modal analysis carried out using computer simulation were used. Spectral analyzes carried out in the working system, regardless of where the measurements were made (hammer, arm tip) showed exactly the same natural frequencies. The graphs for these measurements differ only in the magnitude of accelerations. Table 1 presents the comparison of the natural frequency obtained by experimental and numerical methods together with the error that the calculation model was burdened with. An example of the form of natural frequencies is shown in Fig. 6.

Table 1. Comparison of exemplary natural frequencies

HS Camera (Hz)	FEM (Hz)	Difference (Hz)
1,5	2,6	1,1
13	14,5	1,5
25,25	26,8	1,55
38,75	44,6	5,85
52	56,8	4,8
89,63	86,2	3,43
128,75	128,1	0,65

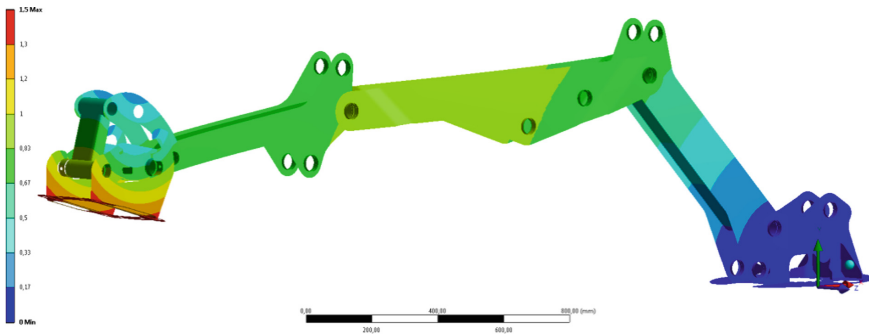


Fig. 6. An example of the deformation of the model

After checking the accuracy of the calculation model, the verification of its response to the displacement was carried out. As a result of applying displacement, the dependence of stresses on the time occurring in the structure during the breaking process was obtained, which is shown in Fig. 7.

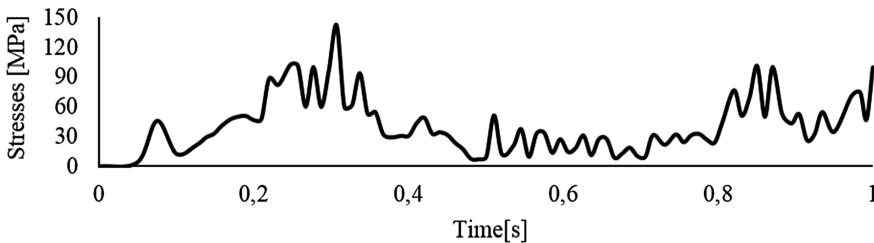


Fig. 7. Dependence of stresses from time in the breaking process

With the applied force in the form of displacement and the analysis of the graph in Fig. 7, it can be concluded that the maximum stresses occur in 0.27 s of simulation. Maximum stresses appeared in the places where the A0 was mounted to the robot structure. This place is stiffened in this type of analysis, so after analyzing the whole structure, it was found that the maximum stresses in the structure amount to 122 MPa and also appeared at the junction of two sheets of the A0. Equivalent (using H-M-H theory) stress distribution are shown in Fig. 8, while the distribution of stress in individual components is shown in Fig. 9.

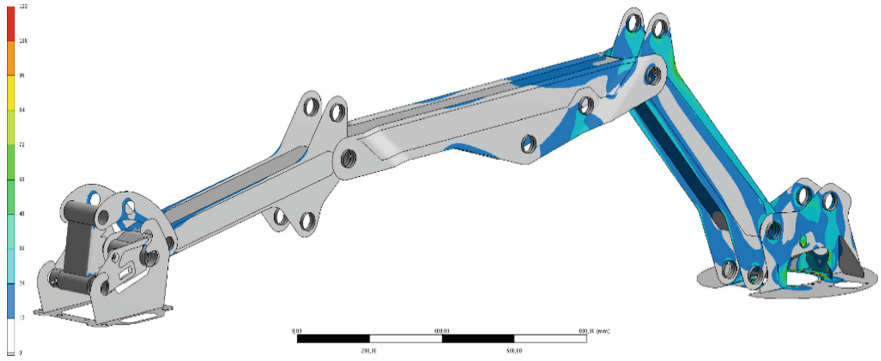


Fig. 8. Equivalent (using H-M-H theory) stress distribution along whole model

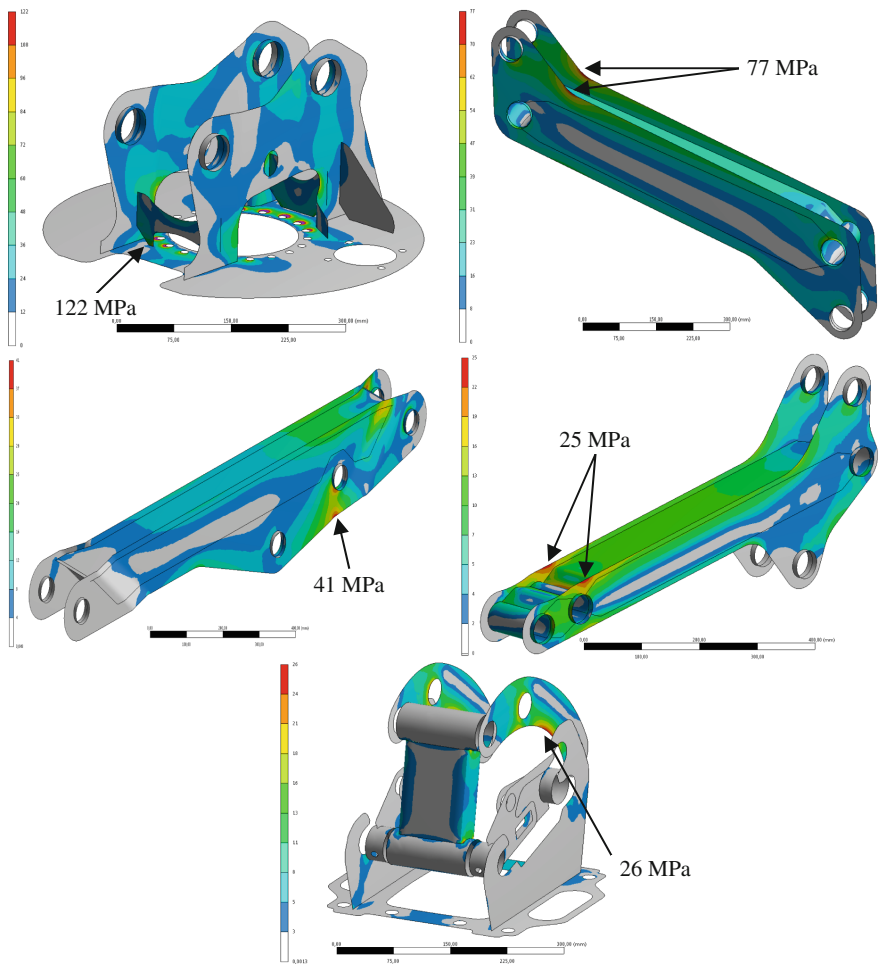


Fig. 9. Equivalent (using H-M-H theory) stress distribution in individual components

5 Summary and Conclusions

Studies using a fast camera to measure displacements and accelerations, allowed to precisely determine the extortion that worked on the robot's arm during its operation. The comparison of the resonant frequency carried out by high-speed camera and simulation confirmed the correctness of the prepared calculation model. Resonance frequencies obtained during experimental research are similar to the resonance frequencies obtained during modal analysis performed by simulations using the Finite Element Method. The computational model contained simplifications so that deviations between the values derived from the numerical analysis and the experiment could be observed.

Analyzing FEM simulations, it can be concluded that the maximum stresses occur in 0.27 s simulation, which is caused by the increase of displacement in the initial violation of the cohesion of the forged material and local cracks. The maximum stresses in the structure occur in the A0, which was an expected effect, because in this place the largest torque acting on the structure is generated.

It can be stated that the numerical and experimental approach gives sufficient information on the state of effort of demolition machine working systems. The use of a high-speed camera to determine the displacement and at the same time to determine the acceleration of the system in order to validate the calculation model limits the number of measuring instruments used to a minimum.

Acknowledgments. The project was carried with the support of the National Centre for Research and Development in Poland under the "Szybka Ścieżka" program no POIR.01.01.01-00-0582/15-00, in cooperation with Advanced Robotic Engineering Ltd. company.

References

1. Derlukiewicz D, Ptak M, Wilhelm J, Jakubowski K (2017) The numerical-experimental studies of demolition machine operator work. In: Lecture notes in mechanical engineering. Springer, pp 129–138
2. Derlukiewicz D, Cieślak M (2017) Study of the causes of boom elements cracking of electric demolition machine with use of experimental and numerical methods. In: Lecture notes in mechanical engineering. Springer, pp 109–119
3. Karliński J, Rusiński E, Lewandowski T (2008) New generation automated drilling machine for tunneling and underg round mining work. *Autom Constr*: 224–231
4. Piszczek K, Walczak J (1982) *Drgania w budowie maszyn*, wyd. 3. Warszawa
5. Rusiński E (2002) Design principles supporting structures of motor vehicles, in Polish. Wrocław
6. Rusiński E, Czmochoński J, Smolnicki T (2000) *Zaawansowana metoda elementów skończonych w konstrukcjach nośnych*. Wrocław
7. Rusiński E, Czmochoński J, Pietrusiak D (2012) Problems of steel construction modal models identification. *Maint Reliab*: 54–61
8. Zienkiewicz O, Taylor R (2006) *The finite element method for solid and structural mechanics*, 6th edn., 3rd repr. edn. Amsterdam
9. Global Construction Robots Market 2016–2020 with Brokk (2016) Fujita & ULC Robotics Dominating. <https://www.businesswire.com/news/home/20160524005815/en/Global-Construction-Robots-Market-2016-2020-Brokk-Fujita>



Analysis of the Causes of Fatigue Cracks in the Carrying Structure of the Bucket Wheel in the SchRs4600 Excavator Using Experimental-Numerical Techniques

Jakub Andruszko, Przemysław Moczko, Damian Pietrusiak^(✉),
Grzegorz Przybyłek, and Eugeniusz Rusiński

Faculty of Mechanical Engineering, Department of Machine Design and
Research, Wrocław University of Science and Technology, Lukasiewicza 7/9,
50-371 Wrocław, Poland
damian.pietrusiak@pwr.edu.pl

Abstract. The article presents design faults related to the carrying structure of the bucket wheel of the SchRs4600 excavator working in the brown coal mine. The authors analyzed cases of damages of this type of structure occurred in the past in such machines. In order to determine the damage of the carrying structure of the bucket-wheel excavator, non-destructive examinations were carried out using visual and magnetic-particle methods. The real loads occurring during operation of the machine in the case of fatigue were also determined. These measurements were used to verify the numerical model. A strength analysis was carried out using the Finite Element Method. The cause of fatigue cracks was determined by measurements and numerical calculations.

Keywords: Mining · Excavator · Bucket-wheel · Cracks ·
Non-destructive testing · Strain gauges · Stress analysis · Finite element method

1 Introduction

One of the basic methods of exploiting mineral raw materials such as brown coal is the opencast method, and its systems have been described in detail in [1]. In order to conduct brown coal mining, specialized machines operating in appropriate systems are used [1].

One of these machines used in open cast mining are bucket-wheel excavators (Fig. 1) and they are a part of a group of machines called basic mining machines. These machines are working in a continuous manner and equipped with a mining head with a number of elements, which are e.g. buckets with teeth. These machines are an integral part of the basic technological system of the open cast mine, where they constitute its first and one of the most important links. The construction of various types of bucket-wheel excavators is practically the same and is based on very similar or even identical functional systems. The construction of various types of bucket-wheel excavators is practically the same and is based on very similar or even identical functional systems. Small differences are described in [2]. One of the basic functional system of a bucket-

wheel excavator is a mining system consisting of a carrying structure, which is a bucket wheel and a mining boom.



Fig. 1. SchRs4600 bucket-wheel excavator

Currently, in the design of carrying structures of basic mining machines, in this case bucket-wheel excavators, the available standards are used. They have been developed based on many years of experience of the manufacturers of these machines. These standards were created at the beginning of the 20th century, and some machines working in brown coal opencast mines were designed according to older standards, which were less precise. The standards have some differences depending on which parts of the world they are used in. Differences between the assumptions occurring in individual standards concerning the design of basic mining machinery are presented in paper [3], where the authors presented differences in terms of static, dynamic and fatigue loads.

Due to the age of these machines, and consequently their large repair history, which is not always correctly carried out, the size of these machines, the complexity of the technological process and the existence of high variable loads that cannot be clearly predicted, these machines are exposed to occurrence of various types of failures [4]. One of the first and at the same time one of the most key elements that is in contact with the material is the bucket wheel of the machine. It is exposed to extreme dynamic loads resulting both from the mining technique, the properties of the material being mined and the hardly-abrasive or non-abrasive materials contained therein. Due to the high variability of loads, sometimes this part of the structure is exposed to various types of failures.

Research articles that have started to appear recently are the result of these failures, and the authors present their individual approaches to determining their causes. One of such failures of the mining system, which was the drive shaft of the bucket wheel in the SRs 2000.32/5.0 + VR92 bucket-wheel excavator, was described in [5], where the